IOP PUBLISHING JOURNAL OF PHYSICS: CONDENSED MATTER

J. Phys.: Condens. Matter **19** (2007) 315218 (22pp) doi:10.1088/0953-8984/19/31/315218

Spin resolved photoelectron spectroscopy of Fe_3O_4: the case against half-metallicity

J G Tobin[1], S A Morton[1], S W Yu[1], G D Waddill[2], I K Schuller[3] and S A Chambers[4]

[1] Lawrence Livermore National Laboratory, Livermore, CA 94550, USA
[2] Department of Physics, University of Missouri-Rolla, Rolla, MO 65409, USA
[3] Department of Physics, University of California-San Diego, La Jolla, CA 92093, USA
[4] Pacific Northwest National Laboratory, Richland, WA 99392, USA

Received 30 October 2006, in final form 11 January 2007
Published 3 July 2007
Online at stacks.iop.org/JPhysCM/19/315218

Abstract

Many materials have been theoretically predicted to be half-metallic, and hence suitable for use as pure spin sources in spintronic devices. Yet to date, remarkably few of these predictions have been experimentally verified. We have used spin polarized photoelectron spectroscopy to study one candidate half-metallic system, Fe_3O_4. Such experiments are normally hampered by difficulties in producing clean stoichiometric surfaces with a polarization that is truly representative of that of the bulk. However, by utilizing higher photon energies than have traditionally been used for such experiments, we can study polarization in 'as received' samples, essentially 'looking through' the disrupted surface.

High quality, strain relieved, *ex situ* prepared Fe_3O_4 films have been thoroughly characterized by diffraction, transport and magnetometry studies of their crystallographic, electronic and magnetic properties. The spectroscopic results are found to agree fairly closely with previously published experimental data on *in situ* grown thin films and cleaved single crystals. However, despite the higher photoelectron kinetic energies of the experiment, it has not been possible to observe 100% polarization at the Fermi level. Hence, our data do not support the claim of true half-metallicity for Fe_3O_4.

(Some figures in this article are in colour only in the electronic version)

1. Introduction

The field of half-metallic ferromagnets has attracted intense theoretical, experimental, and technological interest in the decades since de Groot [1] first postulated the existence of such materials, based upon theoretical band structure calculations of the ferromagnetic Heusler alloy NiMnSb. By definition, such materials possess metallic character for one electron spin

 © 2007 IOP Publishing Ltd Printed in the UK

population and insulating or semiconducting character for the other, and thus exhibit 100% polarization of the conduction band. Much of the interest in such materials stems from the technological potential of half-metals for use as a pure spin sources in future spintronic applications [2], which would fully exploit the electron spin state in addition to its charge to produce innovative, non-volatile, radiation-hard, data processing and storage devices.

Theoretical band structure calculations have now predicted half-metallic character for a wide range of materials. In addition to Heusler alloys [3], these include, perovskites [4, 5], metallic oxides [6] and CMR systems [7]. Despite intense experimental investigation over many years, very few of these theoretical predictions have been verified experimentally [8]. The most compelling evidence to date for half-metallic character has been obtained from Andreev reflection studies of the metallic oxide CrO_2 [9] and spin resolved photoemission studies of the perovskite $LaSrMnO_3$ [10]. However, the latter report has recently been questioned in the literature [11]. The reasons for the absence of 100% polarization in real world systems are many-fold. These include the limitations inherent to the theoretical models that arise from (1) the complex crystallographic structures of many of the candidate materials and (2) the possible presence of strong electron correlation which would severely limit the appropriateness of the standard single-electron picture. Furthermore, significant experimental challenges have also been encountered in studying many candidate half-metallic systems. These experimental limitations include the recurrent issues of stoichiometry, contamination, surface termination, reconstruction [12] and segregation [13]. All of these make it extremely challenging to obtain a surface with a stoichiometric, electronic and magnetic character that truly represents that of the bulk material and is thus suitable for further study using the standard techniques for measuring the polarization of the conduction electrons—Andreev reflection or spin resolved photoemission. These experimental and theoretical difficulties have spurred particular interest in the proposed metallic oxide half-metals CrO_2 and Fe_3O_4. These two oxides have crystallographic structures that are much simpler than that of many of the other candidate materials, making them significantly easier both to model theoretically and to prepare experimentally. Furthermore, both materials have long histories of prior technological use, particularly in the data recording industry, and so their preparation and characteristics are already well understood. Fe_3O_4 in particular can be grown using relatively minor variations on standard deposition techniques, which thus makes it particularly suitable for accelerated integration into potential device physics applications.

In the next several sections of the paper, the following topics will be discussed sequentially: (section 2) historical overview: the structure and magnetism of Fe_3O_4; (section 3) sample preparation; (section 4) experimental details; (section 5) experimental results from 'as received' samples; (section 6) impact of cleaning via ion bombardment; (section 7) temperature dependent spin polarization measurements; (section 8) depth dependent polarization measurements; (section 9) comparison of experimental results to theoretical DOS calculations; and (section 10) summary discussion. In the (section 11) conclusions, it will be described how the experimental results point inevitably to the absence of half-metallicity in Fe_3O_4.

2. Historical overview: the structure and magnetism of Fe_3O_4

At room temperature Fe_3O_4 has a cubic inverse spinel structure in which the larger O ions form a close-packed fcc structure, with the smaller Fe ions occupying two distinct interstitial sites within the O lattice that are normally denoted as A and B. One third of the Fe ions occupy the tetrahedrally coordinated A sites, which consist solely of Fe^{3+} ions, whilst the remaining two thirds occupy the B sites which are octahedrally coordinated and contain both Fe^{2+} and Fe^{3+}

ions arranged in a random distribution. Across a temperature range from 120 K up to the Néel transition at 858 K, the moments within the individual A and B sublattices are ferromagnetically coupled, but in opposite directions. This results in an overall ferrimagnetic character with a net magnetic moment of 4.1 μ_B per formula unit [14]. Theoretical local spin density approximation band structure calculations [6] of this ferrimagnetic phase have predicted that it is half-metallic with a spin up band gap of approximately 0.4 eV and a partially filled metallic spin down t_{2g} conduction band.

One particularly noteworthy feature of Fe_3O_4 is the existence of a Verwey transition [15] at 120 K, which is characterized by an abrupt drop in conductivity by some two orders of magnitude upon cooling through the transition, as well as a pronounced drop in magnetization. The precise nature of this transition has long been the subject of much debate. However Verwey and Haayman [15] have interpreted it as resulting from spontaneous ordering of the Fe B lattice sites leading to a structural transformation from cubic to monoclinic and the closing down of the two-stage electron hopping process between the 2+ and 3+ B lattice sites that forms the primary conduction mechanism above T_v.

The presence of the Verwey transition is of crucial importance for any experimental investigation of the proposed half-metallic character of Fe_3O_4, as it precludes the use of one of the most powerful techniques normally utilized in such investigations: Andreev reflection. These measurements must be performed at temperatures that are significantly below the T_v for Fe_3O_4. Hence, most studies of electron polarization in Fe_3O_4 have focused on using spin resolved photoemission or spin resolved secondary electron spectroscopy. To date, such measurements have yielded highly disparate results in which polarizations at E_f range from +30% [16] to −80% [17] for thin films and −40% [18] to −60% [16] for bulk cleaved single crystals. A number of factors have been invoked to explain the failure to observe −100% polarization in Fe_3O_4, including the presence of strong electron correlation effects [19, 20] and the excitation of spin waves [17]. It is clear than one factor of crucial importance in such measurements is the presence of significant sample preparation and characterization issues such as surface reconstructions [12], surface disorder, surface contamination and interfacial strain [21]. The latter is a particular problem for the type of thin film samples that are of crucial interest for possible spintronic applications and which must generally be grown on an epitaxial substrate. Interfacial strain has been shown to have a dramatic impact on the observed magnetic properties of such samples [21, 22]. Hence, proper characterization and elimination of interfacial strain is vital in any systematic investigation of the polarization of epitaxial thin film Fe_3O_4 samples. Such characterization can be achieved through close monitoring of the sharpness, magnitude and onset temperature of the Verwey transition. Small variations in the observed values from those that are characteristic of bulk single crystals are indicative of (1) the presence of strain, (2) small deviations from stoichiometry, or (3) sample inhomogeneity in the films [23, 24]. Such measurements provide a powerful tool for the characterization of Fe_3O_4 sample quality and are crucial in the preparation of high quality, strain free films for subsequent polarization analysis.

3. Sample preparation

Single-crystal, epitaxial, thin films of Fe_3O_4(001) were prepared by the University of California-San Diego (UCSD) and Pacific Northwest National Laboratory (PNNL), using two slightly different preparation methods. Samples prepared by UCSD were grown by reactive dc sputtering of Fe onto MgO(001) substrates. Deposition was conducted in a partial pressure of O_2 (2% ± 0.2%) at a substrate temperature of 400 °C. The existence of several structurally similar stable iron oxide phases at room temperature necessitates the precise control of gas

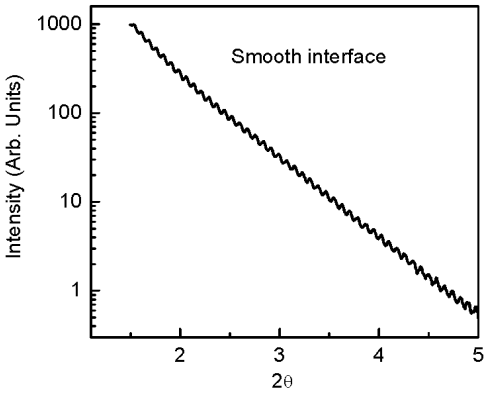

Figure 1. X-ray diffraction scan of Fe_3O_4 thin film grown via the UCSD method shows negligible interfacial roughness.

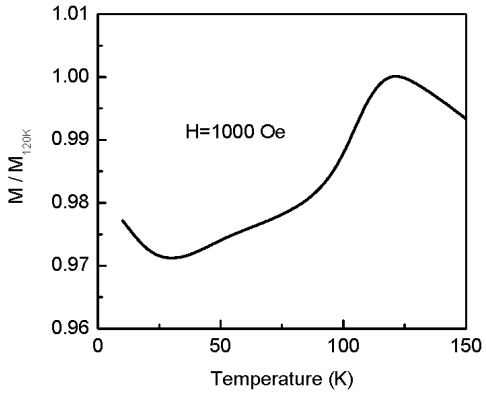

Figure 2. Temperature dependent magnetometry data for strain relieved Fe_3O_4 film grown via the UCSD method; data are normalized to a temperature of 120 K. Note the drop in magnetization occurring at approximately the same temperature as the Verwey transition seen in bulk Fe_3O_4 crystals.

composition and substrate temperature, if the correct stoichiometry and crystal structure are to be achieved. MgO has been widely used as a growth template for Fe_3O_4 as its lattice parameter is almost precisely half that of Fe_3O_4. Although the lattices have a different crystallographic structure, they are both based on an O fcc sublattice which allows for a continuous O structure across the interface. Despite this, such films normally exhibit considerable in plane tensile stress due to the 3% interfacial lattice mismatch. In turn, this leads to anomalous magnetic properties [21, 22] and a suppressed Verwey transition [23], that occurs at a temperature significantly below that normally observed in bulk single crystals. In plane stress was relieved in the UCSD samples by the growth of a 300 Å buffer layer between the MgO substrate and the final 1000 Å Fe_3O_4 layer. Such multilayer samples displayed negligible signs of interfacial roughness and strain when characterized by x-ray diffraction (XRD, figure 1) and reflection high energy electron diffraction (RHEED). They also exhibited pronounced Verwey transitions at temperatures close to those observed in bulk single crystals, as determined by temperature dependent measurements of sample magnetization passing through the transition (figure 2). Furthermore, the magnetization hysteresis loops (figure 3) are square above the Verwey transition temperature, corresponding to the ferrimagnetic coupling regime of the A and B sublattices, in which the two sublattices switch magnetization simultaneously. Below the Verwey transition, the loops become stepped corresponding to weak ferromagnetic coupling of the sublattices. Here, there are separate discrete switching points for the A and B sublattices, occurring at different field strengths, as would be expected from bulk single-crystal Fe_3O_4 samples. Thus, the *ex situ* growth of high quality, strain free, Fe_3O_4 thin films on MgO

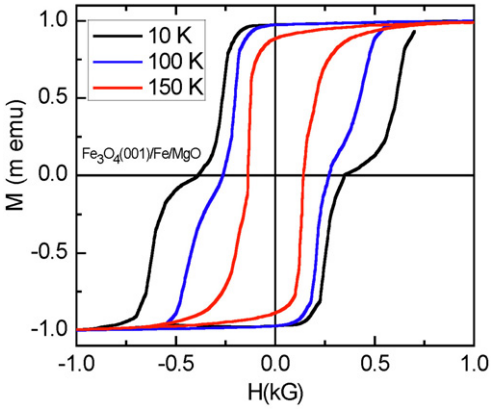

Figure 3. Temperature dependent magnetic hysteresis loops from strain relieved Fe_3O_4 film grown via the UCSD method. Note single switching above the Verwey transition temperature and two-stage switching below it.

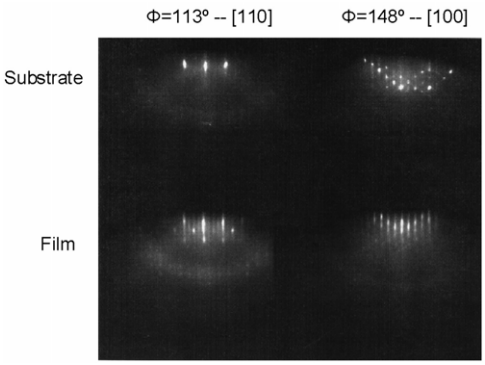

Figure 4. RHEED images from an Fe_3O_4 film grown by the PNNL method compared to equivalent images from the bare MgO substrate.

and the precise characterization of their structural character via x-ray and electron diffraction techniques, combined with magnetometry studies of their Verwey transitions, avoids some of the pitfalls associated with the *in situ* oxidation of single-crystal Fe surfaces [25, 26].

Samples grown at PNNL were prepared in a slightly different manner, by evaporation of Fe at a rate of 0.5 ± 0.1 Å s^{-1}, in the presence of an oxygen plasma. The oxygen plasma was activated by an electron cyclotron resonance source in the manner described elsewhere [12]. Evaporation was again onto Mg(001) substrates and again a buffer layer was used to alleviate interfacial strain. In this case, a somewhat different method was used to obtain high quality strain free samples. Initial growth of the first 1000 Å of Fe_3O_4 was conducted at an elevated temperature of 450 °C, then the temperature was lowered to 250 °C for the final 1000 Å deposition. This preliminary, high temperature growth phase causes out-diffusion of Mg from the substrate [24], into the lower layers of the film. This results in step-flow growth, which relieves interfacial strain, removes defects and produces atomically smooth Fe_3O_4 surfaces as characterized by RHEED (figure 4). Additional *in situ* characterization, by low energy electron diffraction (LEED, figure 5), demonstrated the presence of the characteristic $\sqrt{2} \times \sqrt{2}$ R45° surface reconstruction of Fe_3O_4 [12], with no evidence of any additional contributions from other ordered phases such as Fe_2O_3 or FeO. *In situ* x-ray photoelectron spectroscopy (XPS), conducted with a Scienta 200 analyser, demonstrated that the ratios of the Fe^{3+} and Fe^{2+} contributions to the Fe $2p_{3/2}$ peak and the overall O 1s lineshape are all characteristic of those seen in high quality single-phase Fe_3O_4 samples [12] (figure 6).

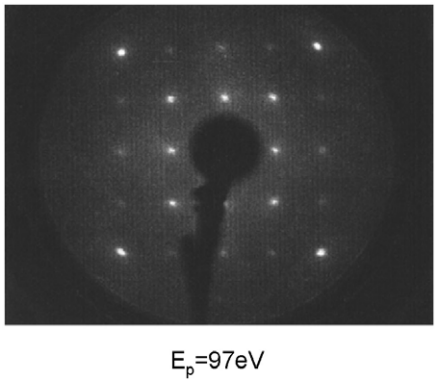

Figure 5. LEED image from an Fe_3O_4 film grown via the PNNL method show the $\sqrt{2} \times \sqrt{2}$ R45° surface reconstruction that is characteristic of a high quality Fe_3O_4 surface. The energy was 97 eV.

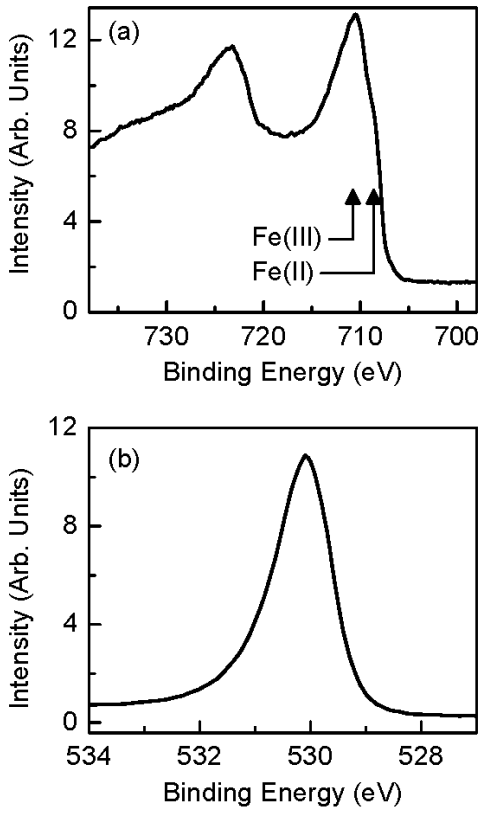

Figure 6. (a) *In situ* XPS spectrum ($h\nu = 1253.6$ eV) of the Fe 2p region taken from a Fe_3O_4 film grown via the PNNL method. Fe^{2+} contribution is visible as a distinct shoulder on the low binding energy side of the Fe^{3+} peak. (b) *In situ* XPS spectrum ($h\nu = 1253.6$ eV) of the O 1s peak region taken from a Fe_3O_4 film grown via the PNNL method.

4. Experimental details

After growth, the samples were transferred *ex situ* to the Beamline 7 SpectroMicroscopy Facility Spin Chamber at the Advanced Light Source. Here were performed further studies

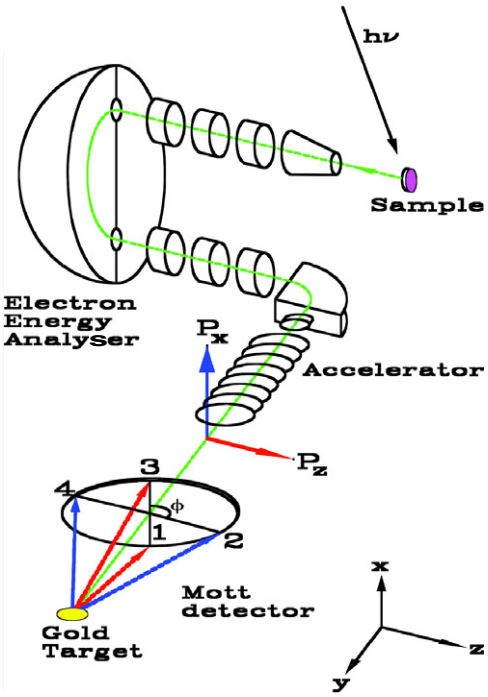

Figure 7. Here is shown a schematic of the energy and spin analyser system. The multichannel detector (no spin) is at the exit plane of the large hemisphere. The multichannel detector has a hole in its centre, which permits electrons to go through it and into the electron optical system. This includes a 90° bend and ends at the Mott detector. The Mott detector measures two components of the spin, along z and x.

using XPS, UPS, x-magnetic linear dichroism in photoemission (MLDAD) and spin resolved photoelectron spectroscopy (SPES). This facility is described in detail elsewhere [27, 28]. The third-generation, high brightness undulator provides a tunable source of 80–1300 eV photons, linearly polarized in the plane of the accelerator. Peak flux from first-harmonic radiation is obtained over an energy range of approximately 80–190 eV and it is this region that provides optimal conditions for SPES and for valence band photoemission. Higher energy fifth-harmonic radiation can also be used for core level XPS, primarily for sample characterization purposes. The XPS measurements were normally conducted at an energy of 1253 eV for comparison with published data from Mg Kα sources. It should be noted that the first-harmonic energy range used for both valence band spin integrated and spin resolved photoemission, and hence both the kinetic energy of the emitted photoelectrons and the resulting experimental sampling depth, are all substantially higher than those commonly used for SPES at most other synchrotron facilities or with traditional noble gas discharge sources.

The emitted photoelectrons are collected by a PHI 10360 SCA hemispherical analyser modified to be capable of operation in both spin integrated (conventional XPS) and spin resolved (SPES) mode [27, 29] (see figure 7). In spin integrated mode, the electrons are detected by a microchannel plate detector situated at the exit plane. In spin resolved mode, the electrons are focused through a central hole in the channel plates and enter a compact 20 kV micro-Mott detector capable of resolving both the in plane and out of plane components of magnetization with a Sherman function of 0.12 and a figure of merit of approximately

10^5. Samples were measured under remnant magnetization conditions, in which they exhibit virtually complete saturation (figure 3). Between successive spectral sweeps the magnetization direction was reversed via pulsed Helmholtz coils. This procedure was used to eliminate any possible contribution from instrumental asymmetries [30].

The experimental resolution for spin integrated XPS, taking into account both photon source and analyser contributions, is as follows: (1) approximately 0.1 eV for valence band and shallow core level studies conducted at energies below 190 eV and (2) 0.8 eV for high energy XPS survey spectra that were conducted at energies above approximately 1000 eV. In spin resolved mode, the experimental resolution is approximately 0.5 eV for energies below 190 eV. The analyser was operated at an angular resolution of approximately $\pm 7^\circ$ resulting in parallel and perpendicular reciprocal space momentum (k) resolutions of 1.56 and 0.1 Å^{-1} respectively. *This large angular acceptance has important implications for the study of half-metals: in order to meet the definition of half-metallicity, the candidate material must exhibit 100% polarization over the entire Brillouin zone.* A spin spectrometer with high angular resolution will only probe a small proportion of the Fermi surface that is highly localized in k-space. Hence, even if the measured polarization in that region reaches 100%, this is not sufficient to confirm the half-metallic nature of the sample. The large angular acceptance of our analyser combined with the relatively large unit cell of Fe_3O_4 ($a = 8.3962$ Å; hence $G = 0.75$ Å), means that we are probing a significant fraction of the Brillouin zone. Thus, our spin resolved band structure measurements are largely free of k dependent angular effects. Furthermore, by varying the photon energy, the region be sampled can moved around in inverse space. Additionally, photoelectron diffraction effects, which can also contribute significantly to the observed signal in a conventional spin integrated photoemission measurement, have previously been demonstrated to have a negligible impact on electron spin polarization as a function of emission angle [31]. Hence the data presented can be considered to be primarily angle integrated in character and truly representative of the of the bulk density of states (DOS).

5. Experimental results from 'as received' samples

As can be seen in figure 8(a), there is a strong spin specific response that was observed in the as received samples. An extensive analysis of surface degradation (figure 8(b)) and contamination (figure 8(c)) effects was also pursued, as will be described next.

Throughout the data acquisition phase samples were maintained at a base pressure of $\sim 5 \times 10^{-10}$. As a result of exposure to atmosphere during the *ex situ* transfer the samples displayed initial 'as received' surface contamination levels of ~0.5–1 nm, as measured by Auger electron spectroscopy (AES) and angle dependent XPS ($h\nu = 1250$ eV). This consisted entirely of C and O species [32]. Comparison of XPS core level ratios (figure 8(c)) shows that C/Fe ratio rises with increasing emission angle, confirming that the C is strongly segregated at the surface. The O/Fe ratio remains approximately constant, indicating that O is present in both the bulk and surface layer, as expected for adventitious surface contamination. Despite this initial surface contamination, XPS measurements of Fe 2p and O 1s (figure 9), conducted on the same sample as for figure 6 but after *ex situ* exposure to atmosphere, reveal that the Fe^{2+} and Fe^{3+} contributions to the Fe 2p lineshape remain essentially unchanged. This result confirms that there has been no significant change in chemical environment as a result of exposure. The O 1s peak also remains largely unchanged although it is considerably broader than before. The broadening of the O 1s peak may be due to the presence of low levels of multiple organic species on the surface. However, it may also simply be a reflection of the somewhat lower resolution of the analyser. UPS measurements of the Fe_3O_4 valence band conducted at a photon energy of

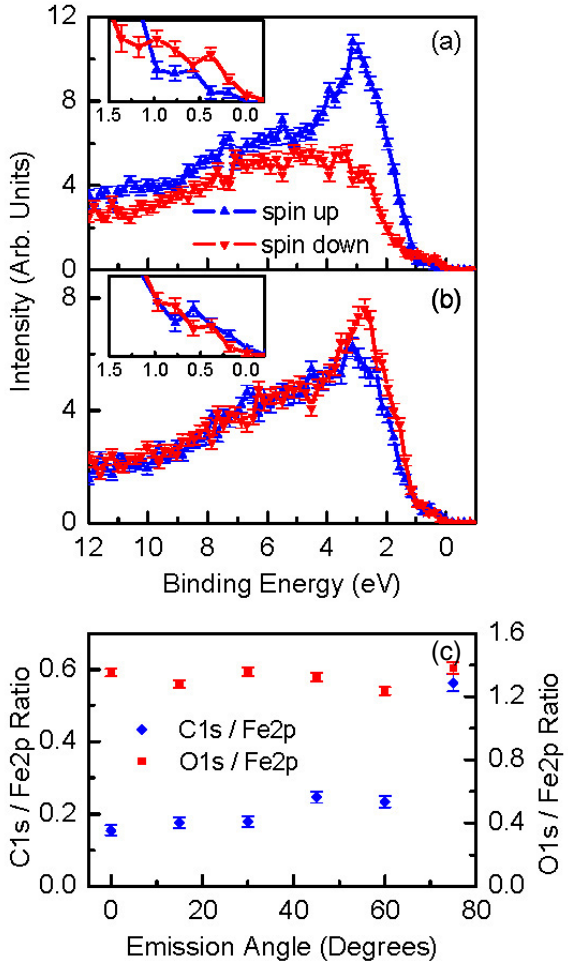

Figure 8. (a) Spin resolved photoemission spectra from (a) 'as received' sample $h\nu = 160$ eV. (b) Spin resolved photoemission spectra from a sample after Ne^+ sputtering, $h\nu = 160$ eV. Note the large effect observed in the as received sample in (a) and the reduction of the effect in (b). (c) Angle dependent XPS measurements of Fe, C and O core level ratios taken from a sample after exposure to air during transfer.

160 eV (figure 10) are also virtually identical to published spectra from *in situ* prepared Fe_3O_4 films [20].

MLDAD measurements conducted on the Fe 3p peak at a photon energy of 160 eV (figure 11) demonstrated the characteristic 'W' form of Fe_3O_4 [26]. The 'W' form arises from the overlapping sets of Fe 3p multiplet structures from the Fe^{2+} (octahedral) and Fe^{3+} (octahedral and tetrahedral) sites. SPES conducted on these 'as received' samples at a photon energy of 160 eV (figure 8(a)) revealed strong positive polarization ($\sim$40%) of the valence band maximum, decreasing to a crossover in the sign of the polarization at approximately 0.9 eV, and strong negative polarization of the Fermi edge ($\sim -40\%$). These data were indistinguishable in both magnitude and form from data reported for both *in situ* cleaved bulk single-crystal Fe_3O_4 samples [18] and *in situ* prepared thin film samples [19]. Together, the results discussed above conclusively demonstrate that exposure to atmosphere during transfer has a negligible impact

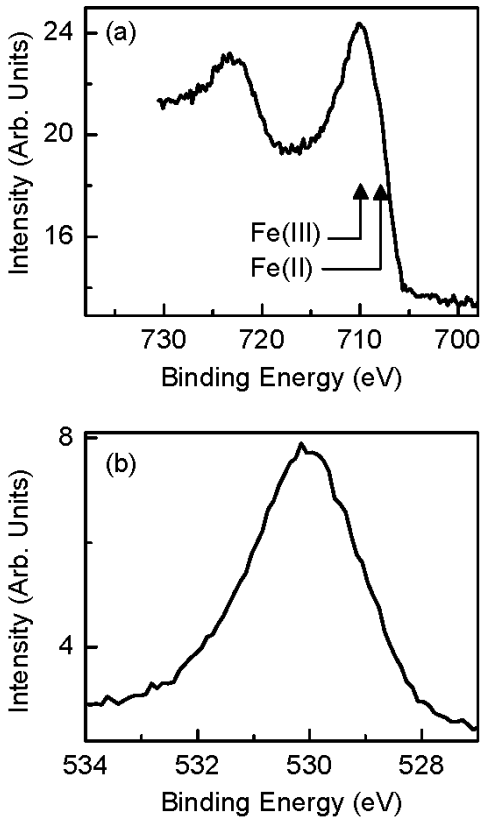

Figure 9. (a) XPS spectrum ($h\nu = 1253.6$ eV) of the Fe 2p region taken from the same sample as for figure 6 after exposure to air during *ex situ* transfer. Fe^{2+}, 3+ ratios remain virtually unchanged indicating no significant change in chemical environment as a result of exposure to the air. (b) XPS spectrum ($h\nu = 1253.6$ eV) of the O 1s peak region taken from same sample as for figure 6 after exposure to air during *ex situ* transfer.

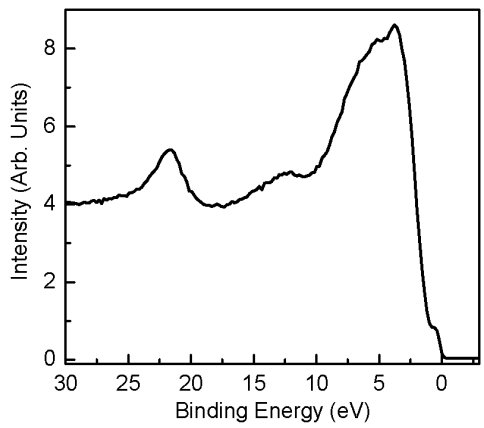

Figure 10. Valence band UPS spectrum of 'as received' Fe_3O_4 film. $h\nu = 160$ eV.

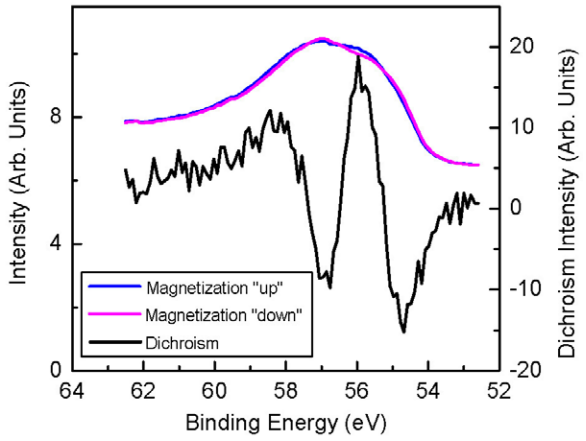

Figure 11. Magnetic linear dichroism spectrum of Fe 3p peak from 'as received' sample, $h\nu = 160$ eV. Here, there is no spin detection, only the dichroic response in spin integrated photoemission, driven by magnetization reversal and the utilization of a chiral configuration of vectors including linear polarization.

on sample quality for high quality, *ex situ* prepared samples, apart from the addition of a thin overlayer of weakly bound adsorbates.

6. Impact of cleaning via ion bombardment

In contrast, *in situ* cleaning processes can have a dramatic impact on the observed magnetic properties of the sample. As can be seen in figure 8(b), 5 min exposure to Ne^+ bombardment or annealing at 500 °C resulted in total loss of the previously strong polarization and even some reversal of polarization [16]. Despite this dramatic impact on the near surface magnetic properties, XPS measurements conducted before and after sample cleaning provided no indication that such significant sample modification had taken place. Hence, spin resolved photoemission provides a powerful surface specific probe of magnetic order. Some success in producing clean surfaces was observed by annealing in a partial pressure of 10^{-6} O_2 for 15 min. This procedure also resulted in an increase in the observed polarization of some 10% in absolute magnitude, for samples showing particularly high levels of initial contamination. However, the risk of significant sample modification either through changes in surface stoichiometry or increased Mg diffusion mobility from the underlying substrate was deemed too great to rely on this procedure. Thus subsequent discussion will focus on measurements of high quality, *ex situ* prepared samples displaying low to moderate levels of as received surface contamination.

7. Temperature dependent spin polarization measurements

The temperature dependence of the near Fermi edge polarization of the 'as received' samples was investigated over a range of temperatures from 100 K up to room temperature using an APD Cryogenics Displex DE202 closed cycle helium cryostat with a quoted accuracy of ± 1 K. Spectra taken at representative temperatures can be seen in figure 12. Little difference could be detected in the spin resolved near Fermi edge spectra across the range of temperatures studied. These results are similar to previous studies [33] using high resolution spin integrated ultraviolet photoemission spectroscopy (UPS), which also demonstrated minimal changes in

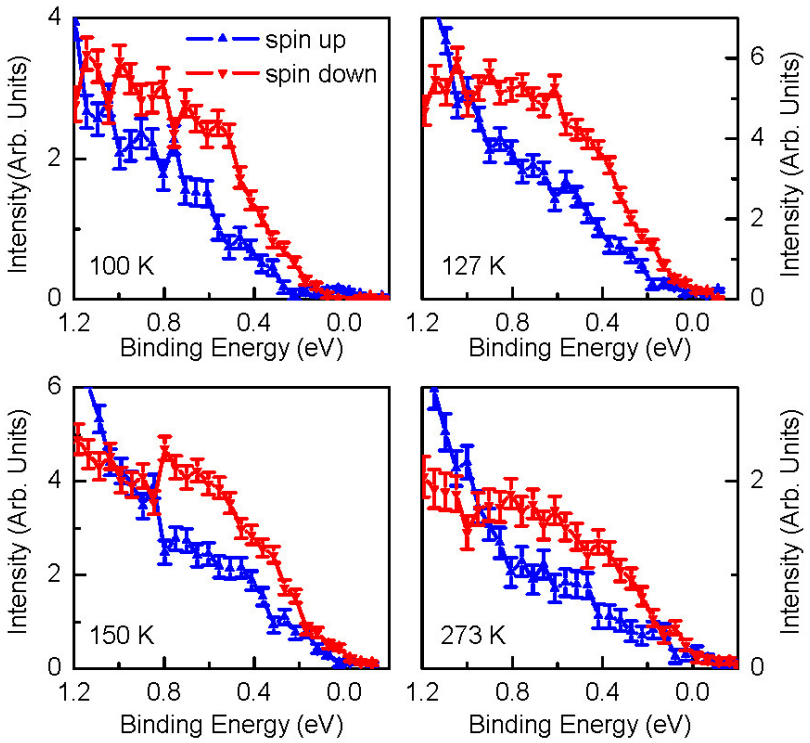

Figure 12. Spin polarized photoemission measurements of the Fermi edge region of Fe_3O_4 conducted at discrete temperatures from 100 K to room temperature, $h\nu = 160$ eV.

the overall structure of the near Fermi edge region. The earlier study did demonstrate a steady decrease in the density of states (DOS) at the Fermi level and the opening up of a band gap of ∼70 meV at 100 K associated with the Verwey metal–semiconductor transition. Although the resolution of our spin resolved study is not sufficient to confirm the existence of such a band gap, there were some indications of a reduced DOS at the Fermi level at the lowest temperatures. In general, it was not possible to acquire spectra at temperatures significantly below 100 K due to a charging problem. This problem maybe indicative of the dramatically decreased conductivity that would be expected to occur below T_v. Our experiments also suggest that the magnitude of the polarization reaches a slight maximum immediately above the Verwey transition, at a temperature of 127 K ± 3 K (figure 13). This temperature is close to that of the isotropic point in which the first-order magnetocrystalline anisotropy constant changes sign [34, 35]. It was not possible to conduct direct measurements of the Verwey transition after exposure to air. However, these observations of effects, which are themselves closely linked to the characteristics of the Verwey transition, together with the earlier spin polarized and dichroism data, provide significant support to the notion that the impact of the exposure to air on the magnetic properties of the sample is negligible.

This suggestion of a maximum in the magnitude of the polarization for temperatures immediately above T_v is also supported by the high resolution spin integrated study. The previous spin integrated work suggests that, as temperatures increases from T_v towards room temperature, the minority spin t_{2g} states at the Fermi level overlap increasingly with the majority e_g states present above 1 eV binding energy. The minority spin t_{2g} states are responsible for

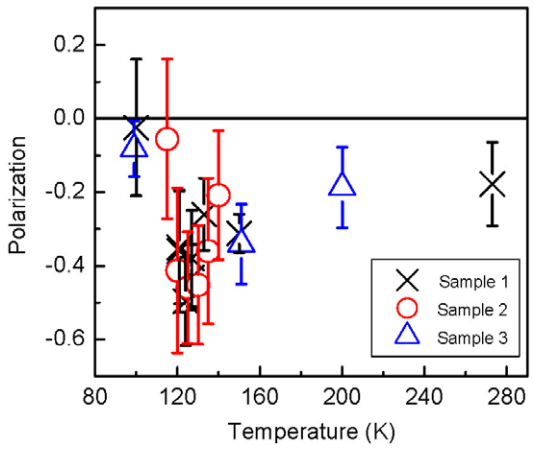

Figure 13. Fermi edge spin polarization as a function of temperature for three 'as received' samples, $h\nu = 160$ eV.

the half-metallic character, so this process would be expected to result in a steady decrease in the observed polarization. Operationally, for all subsequent spin resolved measurements, temperatures around the polarization maximum of 127 K were used.

8. Depth dependent polarization measurements

The magnitude of the observed polarization of the near Fermi edge region of Fe_3O_4 is significantly less than the 100% required for half-metallicity. However, this observation does not necessarily preclude the existence of half-metallic character for bulk Fe_3O_4, as a number of additional factors, both experimental and physical, may act to reduce the observed value from that of the bulk material. The relatively broad energy resolution of the electron analyser with Mott detection means that data are convoluted over a relatively wide region in the vicinity of the Fermi level, not all of which would necessarily possess 100% polarization. This convolution would act to reduce the maximum observed value. Furthermore, the existence of the well documented $\sqrt{2} \times \sqrt{2}$ R45° Fe_3O_4 surface reconstruction [12] strongly suggest the presence of a significant magnetically weak region at the surface. Such reconstructions are readily accounted for by invoking the principle of surface autocompensation [36, 37], i.e. that the most energetically stable surfaces of compound materials with some degree of ionicity are those for which cation (anion) derived dangling bonds are completely empty (or full). However, this principle applies only to semiconducting or insulating surfaces. Such surfaces are driven to achieve autocompensation, through reconstruction, in order to eliminate the surface dipole, which produces a diverging electrostatic energy in the bulk. There is no need to reconstruct in order to autocompensate if a surface is metallic because the surface dipole would be screened by free carriers. The fact that $Fe_3O_4(001)$ exhibits a reconstruction predicted by the surface autocompensation principle for either of the two possible bulk terminations [38, 39] suggests that the surface layer is not metallic, but either semiconducting or insulating. If this layer is magnetically weak (or magnetically dead), it's contribution to the SPES signal would mix with that of underlying layers to yield a SP of less than 100%. In addition, the presence of additional surface contamination in the 'as received' samples will further increase the thickness of the magnetically dead surface layer, to an extent that is dependent on the amount of contamination present.

8.1. Estimation of possible magnetically dead surface layer

If we assume that the surface corruption or reconstruction would tend to destroy the ferrimagnetism associated with the bulk, we can attempt to estimate the underlying spin polarization, by calculating the relative contributions from an unmagnetized surface layer and from an assumed HMFM bulk material below.

$$P' = \frac{\left\{\int_0^t (1/2) I_0 \, \mathrm{e}^{-x/\lambda} \, \mathrm{d}x\right\}_\uparrow - \left\{\int_0^t (1/2) I_0 \, \mathrm{e}^{-x/\lambda} \, \mathrm{d}x + \int_t^\infty I_0 \, \mathrm{e}^{-x/\lambda} \mathrm{d}x\right\}_\downarrow}{\left\{\int_0^t (1/2) I_0 \, \mathrm{e}^{-x/\lambda} \, \mathrm{d}x\right\}_\uparrow + \left\{\int_0^t (1/2) I_0 \, \mathrm{e}^{-x/\lambda} \, \mathrm{d}x + \int_t^\infty I_0 \, \mathrm{e}^{-x/\lambda} \mathrm{d}x\right\}_\downarrow}$$

$$P' = \mathrm{e}^{-t/\lambda}.$$

Here, we have defined I_0 as a normalized emission and $\mathrm{e}^{-x/\lambda}$ is the attenuation, with x being the depth into the sample, λ the mean free path of the outgoing electron [40, 41], and t is the thickness of the surface corruption or reconstruction. Our typical observed polarization is about -40%. If P' is set equal to $|-40\%|$, then $t/\lambda = 0.92$. Since the mean free path is about 5–8 Å, this means that the corrupted/reconstructed layer is on the order of 5–7 Å thick, or roughly 1/2 to 1 unit cell ($a = 8.4$ Å). Thus, it is possible that there is approximately 1/2 to 1 unit cell of the Fe_3O_4 that is being demagnetized by the residual surface contamination or reconstruction. Of course, this is a maximal prediction, based upon the assumption of an underlying bulk polarization of 100%, which may not be justifiable. We will return to this later.

The existence of a magnetically dead surface layer, overlying a more strongly polarized bulk can be confirmed through the use of angle dependent spin polarized photoemission. Due to the previously described angle integrating character of the spin analyser and the relatively large unit cell of Fe_3O_4, such angular dependent measurements will be largely devoid of momentum dependent angular effects. Instead, they will be dominated by the change in the experimental sampling depth as photoelectrons are detected from progressively shallower depths at increasing emission angles, to produce a probe of polarization as a function of depth. This effect can be seen clearly in figure 14 which shows spin polarized spectra of the near Fermi edge region of two typical 'as received' samples. Also shown are their associated spin integrated survey spectra taken at 1253.6 eV, displaying the differing levels of initial surface contamination, as indicated by the strength of the C 1s peak visible at approximately 285 eV. A number of features should be noted. The spin resolved spectra are similar at normal emission, displaying strong negative polarization of the near Fermi edge region, decreasing to a crossover point around 1 eV. As the angle of electron emission is increased, sample A displays a marked decrease in the polarization at the Fermi edge, as might be expected from the presence of a smooth, contiguous and homogeneous unpolarized overlayer. In contrast, sample B displays a greatly reduced angular dependence. Indeed, the changes in polarization are less than the experimental error. These observations can be explained by reference to the initial levels of contamination, as indicated by the spin integrated survey spectra. The level of surface contamination present on sample B is less than one third of that present on sample A. Thus, the demagnetized overlayer, due to possible intrinsic reconstruction and surface disruption from the contamination, is much larger on sample A. Hence, the diminution of the spin polarization with increasing off-normal angle is greatly accelerated in sample A relative to sample B.

This approach can be independently corroborated, by studying how the polarization of the near Fermi edge region changes as a function of photon energy (figure 15). Decreasing the photon energy also changes the electron attenuation length in a manner analogous to that of increasing the emission angle. The range of electron probe depths accessible by changing the photon energy is not as great as those accessible via changes in electron emission angle, and the picture is further complicated by the changes in atomic cross sections, which also occur

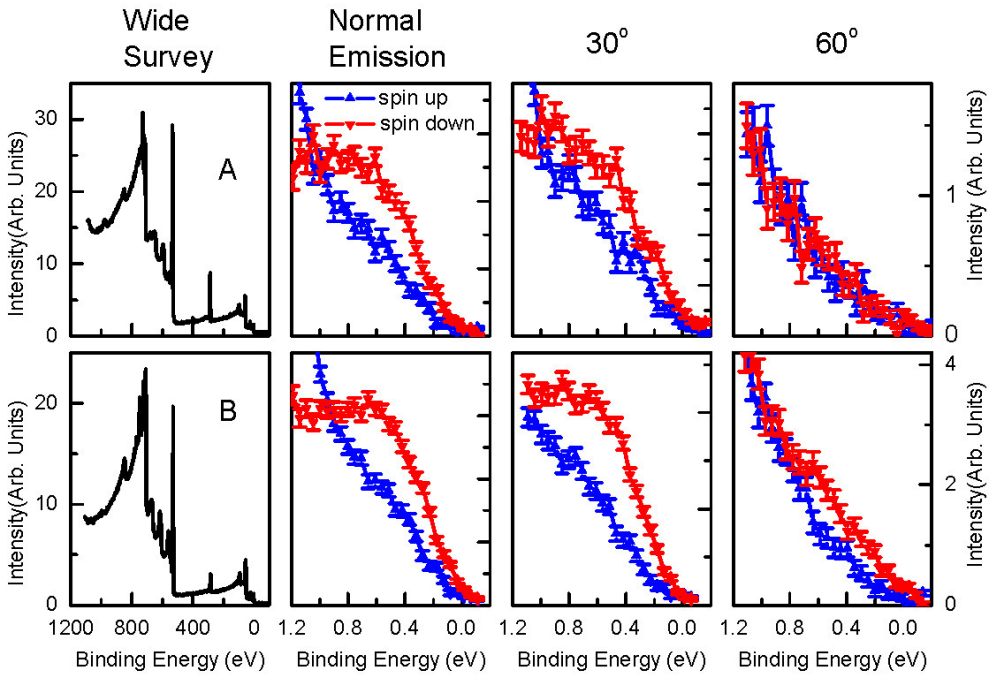

Figure 14. Angle dependent spin resolved spectra of the near Fermi region, conducted at 0°, 30° and 60° off normal emission, for two different 'as received' samples, at $h\nu = 160$ eV. Also shown are the corresponding XPS survey spectrum, illustrating the relative levels of surface contamination.

as a function of photon energy. (Although, the relative contributions of Fe, C, and O remain approximately constant across this energy range [42].) However, despite these limitations, such a study does allow an independent estimate of the thickness of the magnetically dead surface layer and hence to further constrain the possible range of the underlying bulk polarizations. We will return to these subjects below.

8.2. Quantitative model of a magnetically dead surface layer

The angular dependence of the polarization can be considered in a more quantitative manner. This would enable one to estimate the underlying bulk polarization of the Fe_3O_4 samples, once the presence of the magnetically dead (nominally paramagnetic) surface layer, formed from the combined effects of surface reconstruction and surface contamination, was taken into account. The polarization is derived from the up and down components [30, 43] in the manner described in equation (1)

$$P = \frac{I^+ - I^-}{I^+ + I^-}. \tag{1}$$

However, in the case of a material possessing a magnetically distinct surface layer, the spin up and down populations can be thought of as having two separate contributions, derived from the underlayer (i) and overlayer (j), as shown in equation (2).

$$\begin{aligned} I^+ &= i^+ + j^+ \\ I^- &= i^- + j^- \end{aligned} \tag{2}$$

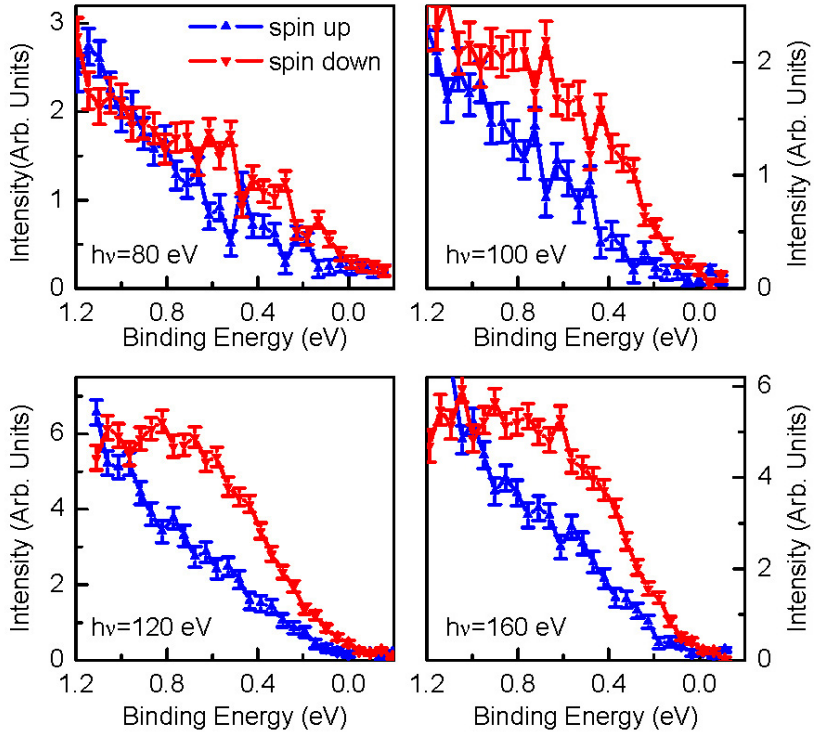

Figure 15. Photon energy dependent spin resolved spectra of the near Fermi edge region conducted at normal emission. Samples are the same as those used in figure 14.

where

$$i = i^+ + i^-$$
$$j = j^+ + j^- \tag{3}$$

$$p = (i^+ - i^-)/(i^+ + i^-). \tag{4}$$

From these it is possible to extract the component, p, due solely to the underlying bulk material (4). Assuming that the overlayer is magnetically dead, and hence $j^+ = j^-$, then

$$p = P\left(1 + \frac{j}{i}\right) \tag{5}$$

and from standard overlayer attenuation theory

$$j = j_0(1 - \mathrm{e}^{-z/z_0})$$
$$i = i_0\mathrm{e}^{-z/z_0} \tag{6}$$

where z is the electron path length and z_0 is the electron escape depth. If d is the film thickness and θ is the emission angle then

$$z = \frac{d}{\cos\theta}. \tag{7}$$

Hence substituting into (5) and defining the parameters ρ and n,

$$\rho = \frac{j_0}{i_0}$$
$$n = \frac{z}{z_0}. \tag{8}$$

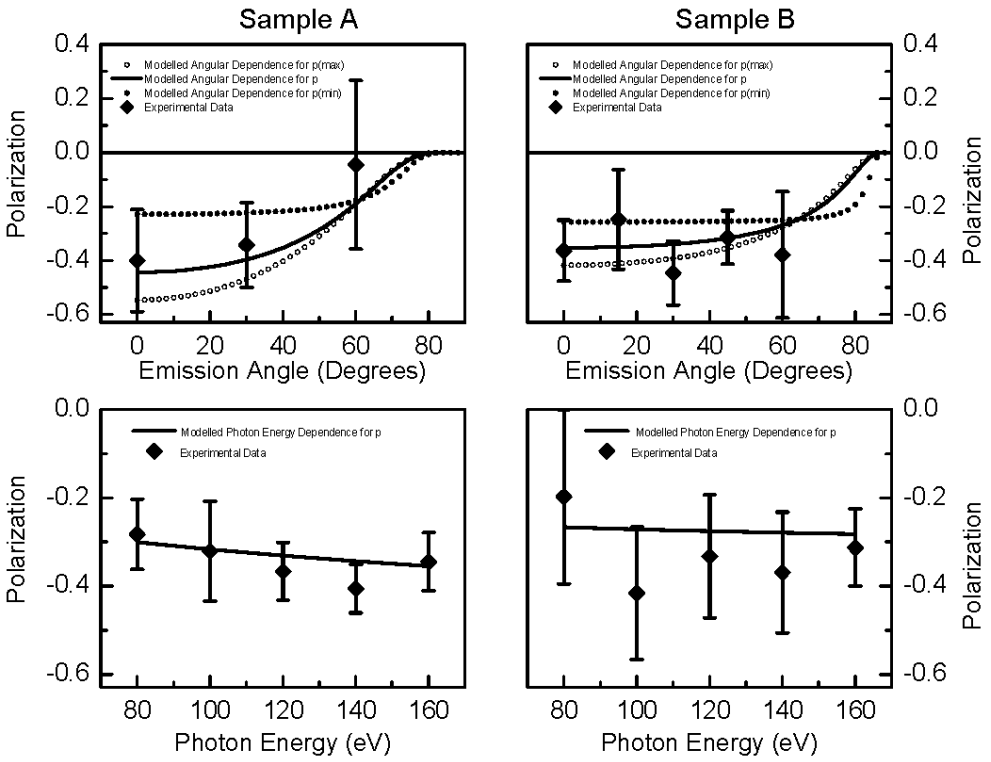

Figure 16. Experimental values for the polarization of two samples (A, B) as a function of both emission angle and photon energy. These are shown together with the calculated curves of what the angular dependence would be for (1) best fit, (2) maximum and (3) minimum values of the underlying polarization, as determined from our substrate/overlayer model.

It is possible to obtain a linear relationship for the underlying polarization, expressed as an inverse linear function of both the observed polarization and the film thickness, where $y = mx + b$ is the standard form for a line.

$$\begin{array}{ccccccc} \dfrac{1}{P} & = & \dfrac{\rho}{p} & \mathrm{e}^{n} & + & \left(\dfrac{1-\rho}{p}\right) \\ \downarrow & & \downarrow & \downarrow & & \downarrow \\ y & & m & x & & b. \end{array} \tag{9}$$

Thus, assuming that the overlayer is indeed completely demagnetized, the underlying polarization, excluding scattering in the overlayer, can be extracted from the least squares fit to a plot of $1/P$ versus e^{n}.

$$p = \frac{1}{m+b}. \tag{10}$$

The results of this analysis can be seen in figure 16, which shows the experimental values for the two samples as a function of both emission angle and photon energy. Also plotted are the calculated curves of what the angular dependence would be for (1) best fit, (2) maximum and (3) minimum values of the underlying polarization as determined from our substrate/overlayer model. Experimental data are obtained by averaging the polarization over a binding energy

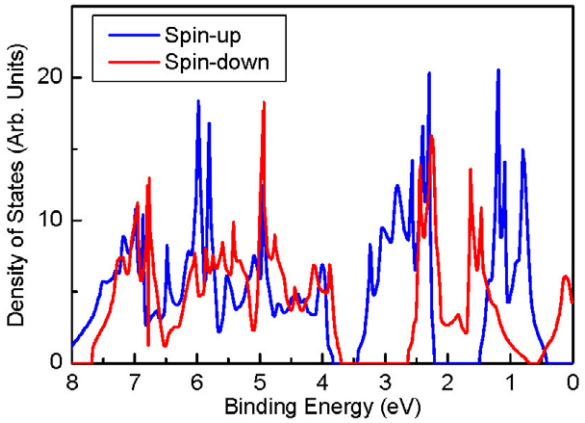

Figure 17. Theoretical spin resolved density of states of Fe_3O_4 (after Zhang and Setpathy [6]).

range of 0–0.2 eV, to reduce the statistical error involved. This model predicts an underlying bulk polarization for Fe_3O_4 of

$$p_{\text{bulk}} = -65\% \pm 35\%.$$

The rather broad error bars are a result of the broad minimum in the model. However, the results do indeed suggest that the underlying bulk polarization of Fe_3O_4 is significantly higher than that which has typically been measured in surface sensitive spectroscopies. In these measurements, the magnitude of the observed polarization is reduced from it's 'true' value, by the presences of a non-magnetic surface layer. It is also possible that experimental factors tend to reduce the observed polarization, such as the effects of finite analyser energy resolution or final state effects. Nevertheless, based upon these angular and energy dependences, there remains only a small chance that Fe_3O_4 may indeed be half-metallic in the bulk. Below, in the conclusions section, we will return to a discussion of what this measured polarization of -65% may mean.

9. Comparison of experimental results to theoretical DOS calculations

Once the physical and experimental effects discussed are properly taken into account a direct comparison can then be made between theoretical, spin dependent band structure models and experimental spin resolved valence band spectra. The spin dependent, valence band density of states of magnetite has been modelled by Zhang and Setpathy [6] using a local spin density approximation approach (figure 17). These calculations predict the presence of a majority spin band gap at E_f extending to a binding energy of approximately 0.4 eV. Hence, the majority spin population is predicted to be insulating in character. In contrast, the minority carriers possess a metallic character with states derived predominantly from the Fe 3d t_{2g} bands of the B lattice sites present at the Fermi level. This model predicts -100% electron polarization at the Fermi level (and thus half-metallicity in Fe_3O_4). The model also predicts the presence of a 1 eV wide band gap in the minority states at a binding energy of 3 eV, resulting in $+100\%$ polarization of the valence band maximum.

However, before a direct comparison can be made between these theoretical band structure calculations and the experimental data reported here, the experimental and physical effects discussed previously must be taken into account. The effects of finite analyser resolution, surface imperfections, and differing photoelectron cross sections must be introduced into the

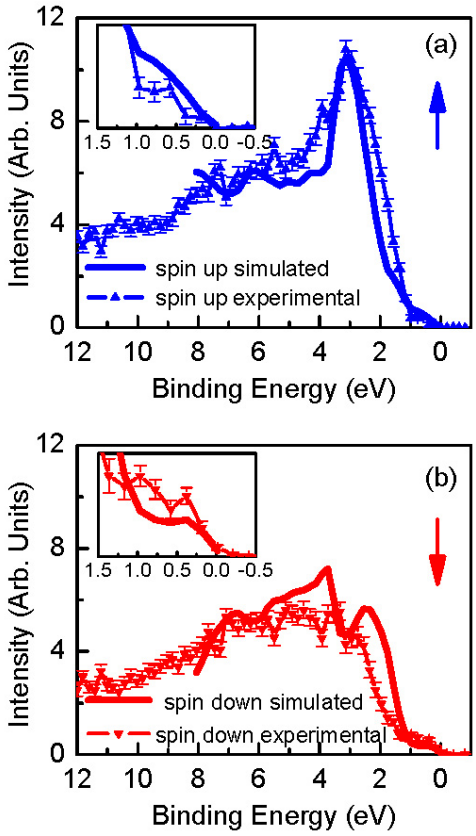

Figure 18. Comparison of experimental spin up (a) and spin down (b) spectra with simulated spectra derived from the theoretical band structure of half-metallic Fe_3O_4. The key operations employed upon the theory plots from figure 17 include broadening and scaling down the spin up peak at a binding energy of 3 eV to match the experimental curve. This is tantamount to reducing the polarization.

calculations in order to produce 'simulated' spin resolved spectra that facilitate comparison with the experimental data.

This analysis procedure and the calculation of simulated spin up and spin down spectra has been discussed in greater detail by the authors elsewhere [44]. The result of this process can be seen in figure 18.

As can be seen there is strong agreement between the experimental data and the simulated spectra derived from theoretical first principles calculations, once the broadening and down-scaling operations have been performed. The simulated spectra display both the correct overall envelopes as well as reproducing specific features of the spin resolved spectra such as the strong majority peak at 3 eV, the reversal of polarization at approximately 1 eV and the strongly negatively polarized Fermi region, which exhibits a polarization of about -40%. However, the magnitude and variations of the experimentally measured spin polarized spectra in the regions of 0.5–2.0 eV and 4.0–5.0 eV binding energy are significantly different than the predictions of the theory, even with the broadening and down-scaling corrections. Hence, although the experimental and theoretical polarizations are actually in general agreement once corrections for the effects of the demagnetized surface region are implemented, a detailed comparison still

indicates significant disparities. This result suggests that while the single-electron results of Zhang and Satpathy [6] are on the right track and almost quantitatively correct, something additional is going on the valence bands. This will be addressed below.

10. Summary discussion

The experiments have demonstrated the feasibility of using well characterized, high quality, strain relieved, *ex situ*-prepared samples to investigate the spin resolved band structure of Fe_3O_4. Measurements conducted with a variety of spectroscopic and magnetic probes demonstrates that while exposure to air results in the formation of a surface layer of adventitious hydrocarbons, it leaves the chemical, electronic and magnetic properties of the samples completely unchanged. Moreover, the observed dichroic properties, polarization at the Fermi energy and band structure of 'as received' Fe_3O_4 sample has been shown to be consistent with that of *in situ* grown thin film samples and cleaved single crystals. The use of higher photon energies to conduct the valence band spectroscopy allows us to probe through this adventitious layer and removes the necessity for potentially damaging cleaning processes, which have been show to significantly impact surface magnetism.

Temperature dependent polarization measurements have shown that the polarization is largely independent of temperature over a temperature range for the Verwey transition up to room temperature. However, it does pass through a maximum amplitude at a temperature of 127 K, which is linked to changes in the first-order magnetocrystalline anisotropy constant.

The measured polarization has been shown to be significantly impacted, by the unavoidable presence of a magnetically dead surface layer. Hence, obtaining a surface with a polarization that is truly representative of that of the bulk material is not feasible by any conventional sample preparation techniques. However, by probing the spin resolved band structure of 'as received' samples without attempting to further modify the surface in any way, and by using photons of a higher energy than conventionally used for spin resolved photoemission, we can probe through this disrupted surface layer. By combining this approach with theoretical predictions, we obtain an estimate of the polarization of the underlying bulk material. The spin polarized spectra of these 'as received' samples have been compared to those generated from an existing theoretical model which predicts half-metallic character for Fe_3O_4. These have been shown to be in general agreement once the effects of finite analyser energy resolution, surface imperfections, and photoelectron cross sections are included, but with a polarization magnitude reduced significantly from 100%.

11. Conclusions

The salient results are as follows:

(1) The measured polarization at the Fermi edge of the 'as received' samples was approximately -30% to -40%.
(2) Using take-off angle and photon energy variations to probe the Fermi edge polarization of the underlying bulk material, a bulk polarization value of -65% was obtained.
(3) Comparing simulated spectra based upon a single-electron model to the experimental spectra produced near quantitative agreement, but nagging discrepancies remain.

All of this points to something going on beyond the prediction of -100% polarization from a single-electron picture. This result is seemingly in contradiction with the experimental result of Dedkov *et al* [17], who report the observation of -80% polarization at the Fermi

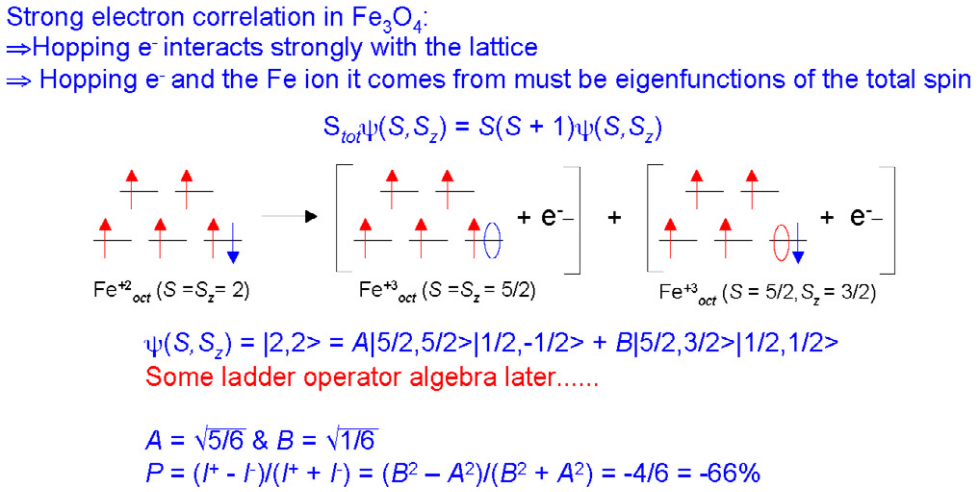

Figure 19. Spin polarization argument following Alvarado and Bagus. See [46].

level. However, these measurements were taken with He I (21.22 eV) and 3° angular resolution. Under these conditions, one is not averaging over the Brillouin zone but is instead susceptible to band effects. As discussed above, averaging over the zone is very important. Half-metallicity requires that the entire density states have one spin only. Observing a high polarization at a single spot in the BZ has been observed before in non-HMFM systems [45]. So its observation by Dedkov *et al* at a single angle is NOT a proof of HMFM in Fe_3O_4.

The obvious candidate is electron correlation. Interestingly, Alvarado and Bagus [46] addressed this issue in 1978, and predicted that the photoelectron spin polarization for a high spin state of d^6 character would be $-2/3 = -66.7\%$ (figure 19). This is embarrassingly close to the determination above for the underlying bulk polarization of -65%. (It should also be noted that measurements performed by Vescovo *et al* [47] using the PNNL type of samples produced a polarization value of -50%, qualitatively supporting our values of -30% to -40% and -65%.) The possibility does remain that finite temperature effects (e.g. magnon band structure, [48]) are the cause of the reduction of the magnitude of the spin polarization below 100%. Unfortunately, measurements nearer to 0 K are an impossibility, because of the Verwey transition in Fe_3O_4. Our experimental results are consistent with the prediction of electron correlation effects. In any case, all of the evidence in our study indicates a reduction of the magnitude the Fermi level polarization, so that the desired value of -100% polarization is not achieved. Fe_3O_4 is not a half-metallic ferromagnet.

Acknowledgments

This work was performed under the auspices of the US Department of Energy, by the University of California Lawrence Livermore National Laboratory under contract W-7405-Eng-48. Work that was performed by LLNL and UMR personnel was supported by the Office of Basic Energy Science at the US Department of Energy. The ALS and the Spectromicroscopy Facility have been built and operated under funding from the Office of Basic Energy Science at DOE. Work at UCSD is supported by DOE. Work at PNNL is supported by the Offices of the Biological and Environmental Research and Basic Energy Sciences at DOE.

References

[1] de Groot R A *et al* 1983 *Phys. Rev. Lett.* **50** 2024
[2] Wolf S A and Treger D 2000 *IEEE Trans. Magn.* **36** 2748
[3] Helmholdt R B *et al* 1984 *J. Magn. Magn. Mater.* **43** 249
[4] Jin S *et al* 1994 *Science* **264** 413
[5] deBoer *et al* 1997 *Solid State Commun.* **102** 621
[6] Zhang Z and Satpathy S 1991 *Phys. Rev.* B **44** 13319
[7] Pickett W E and Singh D J 1996 *Phys. Rev.* B **53** 1146
[8] Kamper K P 1987 *Phys. Rev. Lett.* **59** 2788
[9] Ji Y *et al* 2001 *Phys. Rev. Lett.* **86** 5585
[10] Park J-H *et al* 1998 *Nature* **392** 794
[11] Dulli H *et al* 2000 *Phys. Rev.* B **62** R14629
[12] Chambers S A and Joyce S A 1999 *Surf. Sci.* **420** 111
[13] Bona G L, Meier F and Taborelli M 1985 *Solid State Commun.* **56** 391
[14] Kakol Z and Honig J M 1989 *Phys. Rev.* B **40** 9090
[15] Verwey E J and Haayman P W 1941 *Physica* **8** 979
[16] Aeschlimann M *et al* 1987 *Helv. Phys. Acta* **60** 794
[17] Dedkov Y S, Rüdiger U and Güntherodt G 2002 *Phys. Rev.* B **65** 064417
[18] Alvarado S F *et al* 1975 *Phys. Rev. Lett.* **34** 319
[19] Huang D J *et al* 2002 *Surf. Rev. Lett.* **9** 1007
[20] Huang D J *et al* 2002 *J. Magn. Magn. Mater.* **239** 261
[21] Margulies D T *et al* 1996 *Phys. Rev.* B **53** 9175
[22] Margulies D T *et al* 1997 *Phys. Rev. Lett.* **79** 5162
[23] Lind D M *et al* 1992 *Phys. Rev.* B **45** 1838
[24] Anderson J F *et al* 1997 *Phys. Rev.* B **56** 9902
[25] Kim H-J, Park J-H and Vescovo E 2000 *Phys. Rev.* B **61** 15284
[26] Kim H-J, Park J-H and Vescovo E 2000 *Phys. Rev.* B **61** 15288
[27] Tobin J G *et al* 1998 *MRS Symp. Proc.* **524** 185
[28] Denlinger J D *et al* 1995 *Rev. Sci. Instrum.* **66** 1342
[29] Tobin J G and Schumann F O 2001 *Surf. Sci.* **478** 211
[30] Johnson P D 1997 *Rep. Prog. Phys.* **60** 1217
[31] Waddill G D *et al* 1994 *Phys. Rev.* B **50** 6774
[32] Morton S A *et al* 2000 *Bull. Am. Phys. Soc.* **45** 644
[33] Chainai A *et al* 1995 *Phys. Rev.* B **51** 17976
[34] Gridin V V, Hearne G R and Honig J M 1996 *Phys. Rev.* B **53** 15518
[35] Stacey F D and Banerjee S K 1974 *The Physical Principles of Rock Magnetism* (New York: Elsevier)
[36] Pashley M D 1989 *Phys. Rev.* B **40** 10481
[37] LaFemina J P 1994 *Crit. Rev. Surf. Chem.* **3** 297
[38] Chambers S A, Thevuthasan S and Joyce S A 2000 *Surf. Sci.* **450** L273
[39] Stanka B *et al* 2000 *Surf. Sci.* **448** 49
[40] Somorjai G A 1981 *Chemistry in Two Dimensions: Surfaces* (Ithaca, NY: Cornell University)
[41] Ertl G and Kueppers J 1974 *Low Energy Electrons and Surface Chemistry* (Weinheim: Verlag Chemie)
[42] Yeh J J and Lindau I 1985 *At. Data Nucl. Tables* **32** 1
[43] Kessler J 1985 *Polarized Electrons* (Berlin: Springer)
[44] Morton S A *et al* 2002 *Surf. Sci. Lett.* **513** L451
[45] Hochstrasser M, Tobin J G, Rotenberg E and Kevan S D 2002 *Phys. Rev. Lett.* **89** 216802
[46] Alvarado S F and Bagus P S 1978 *Phys. Lett.* A **67** 397
[47] Vescovo E, Kim H J, Ablett J M and Chambers S A 2005 *J. Appl. Phys.* **98** 084507
[48] Dowben P A and Skomski R 2004 *J. Appl. Phys.* **95** 7453
Dowben P A and Jenkins S J 2007 The limits to spin-polarization in finite-temperature half-metallic ferromagnets *Frontiers in Magnetic Materials* ed A V Narliker (Berlin: Springer)